Design and Simulation of Ultra low loss Spiral Delay line for Integrated Optical Coherence Tomography

Bhawna Sharma (bhawnasharma.110391@gmail.com)
DIT University
Kamal Kishor
Delhi Technological University
Amrindra Pal
DIT University
Sandeep Sharma
Chang Gung University
Roshan Makkar
Society for Applied Microwave Electronics Engineering and Research

Original Research

Keywords: Spiral delay line, OCT, silicon nitride, integrated optics

Posted Date: February 4th, 2021

DOI: https://doi.org/10.21203/rs.3.rs-171702/v1

Version of Record: A version of this preprint was published at Optical and Quantum Electronics on July 14th, 2021. See the published version at https://doi.org/10.1007/s11082-021-03047-y.

Design and Simulation of Ultra low loss Spiral Delay line for Integrated Optical Coherence Tomography

BHAWNA SHARMA,[1,*] KAMAL KISHOR,[2] AMRINDRA PAL,[1] SANDEEP SHARMA,[3] AND ROSHAN MAKKAR[4]

[1]Electronics & Communication Engineering, DIT University, Dehradun-248009, Uttarakhand,
[2]Department of Physics, Delhi Technological University, (Formerly Delhi College of Engineering), Bawana road, Delhi-110042, India
[3]Centre for Reliability Sciences and Technology, Department of Electronics Engineering, Chang Gung University, Taoyuan, 33302, Taiwan
[4]Photonics Division, Society for Applied Microwave Electronics & Engineering Research, IIT Bombay Campus, Powai, Mumbai, Maharashtra, India

Abstract: We report a design of 55 cm long spiral delay line at 850 nm wavelength. Propagation characteristics were simulated and analysed with fully vectorial Eigen Mode Expansion (EME) method. Bending losses were calculated and analysed for the optimization of minimum bending radius for reported structure. We have also simulated and analysed excess loss for a broadband of 200 nm at 850 nm operating wavelength. An excess loss of less than 0.2 dB is reported for the structure over the entire bandwidth range. The structure was further simulated for individual Transverse Electric (TE) and Transverse Magnetic (TM) modes and the analysis showed better results for TM mode. Reported structure is easy to fabricate, ultra-low loss and also broadband over 200 nm with a foot print of only 6×6 sq. mm. So, this design will improvise the reference arm section and will enhance the depth scanning of integrated optics based optical coherence tomography system**.**

Keywords: Spiral delay line, OCT, silicon nitride, integrated optics

1. Introduction

Photonic integrated components have recently gained wide interest in medical and industrial applications [1][2]. One such biomedical application is optical coherence tomography (OCT). OCT is a non-contact imaging technique which works on the principle of low coherence interferometry [3]. The generic OCT system consists of a broadband monochromatic light source which is directed on to a 2×2 fibre optic coupler in order to split the incident power evenly into the sample and reference arm. Light from the reference arm is sent upon a reference delay and redirected back whereas light from the sample arm is sent to a scanning mechanism which is structured to focus the beam on the sample. The recombined light from the sample and reference arms gives rise to interference pattern only when constructive interference takes place. The scanning depth of sample is controlled by the delay in the reference arm for deep scanning [4].

Optical delay lines (ODL) are important components which are used to provide a timed delay in a system. When these ODLs are implemented using integrated chips they show various advantages such as reduced cost, size, weight and power consumption [5]. They have various applications such as optical beam forming networks for antenna arrays, imaging processing units, radio on fibre links and devices, OCT systems and sensing units. There are different techniques to obtain optical delay in photonic integrated circuits such as integrated grating [6] delay lines(IGDL) wherein the spatial structure or refractive index parameter undergoes a periodic change mainly by modulating its structural parameters such as waveguide width and height or by modulating its effective refractive index [7], photonic crystal waveguides (PhCWs) based delay lines in which the photonic crystals consist of periodic optical micro and nano structures resulting in manipulation of light propagation while maintaining its efficiency [8], micro ring resonators(MRR) having the advantage of compact size and scalability consists of cascaded optical ring resonators for obtaining tuneable delay lines mainly in side coupled integrated space sequence of resonators(SCISSSOR) or coupled resonator optical waveguides (CROW) fashion and optical waveguide spiral delay lines which are simple length dependent delay structures that can be implemented using various material technologies such as Indium Phosphide (InP), silicon nitride (Si_3N_4) and silicon on insulator(SOI) [9].

While PhCWs offer wide bandwidth but incur high propagation losses, MRRs offer small foot print but usually have narrow bandwidth and bandwidth delay product is rather small. IGDLs offer compact resonant delay lines but fabrication is rather challenging and insertion loss is also high. Spiral delay lines are most promising candidate as they offer optimal area utilization with low loss, large bandwidth and does not require any external control. Moreover, these delay lines can be easily integrated with other components.

Various components in OCT system can be integrated on a chip so as to miniscule the existing fibre optic based OCT system. Numerous research groups have designed various components on an integrated optics platform for

OCT system. Yurtsever et al. reported a Mach-Zehnder interferometer (MZI) based integrated circuit consisting of numerous y-splitters and 190mm reference arm using Si_3N_4 / SiO_2 waveguides at 1320 nm. Upon its realization, the system was used to scan different layers of finger tip [10]. Cascaded MZI with tunable couplers-based delay line with delay tuning range of 124 ps was reported at 1550 nm central wavelength [11]. Recently cascaded MRRs on Si_3N_4platform was proposed. These structures showed a maximum delay tuning range of 394.6 ps @ 2GHz bandwidth using continues tuning method [12].

In this paper, a spiral reference ODL for depth scanning in integrated optics-based OCT system is reported. This reference delay line is designed for 850 nm central wavelength using Si_3N_4 and SiO_2 waveguides. The proposed structure is compact, low loss, broadband and long enough to provide deep scanning for OCT system. This structure was modelled for FV mode type and was found to be broadband over 200 nm bandwidth with an excess loss of 0.17dB. The structure was further simulated for individual TE and TM mode and minimum bending radius is also calculated. Comparative analyses for all three modes were done and it is found that TM mode being the most promising candidate with minimal propagation losses. The reported compact reference delay line upon realization along with integrated directional coupler [10-11] will completely replace the bulky fiber-based interferometer in a Fourier domain OCT system.

2. Waveguide design and modelling

The reported spiral structured optical delay line is designed for integrated optics OCT system at 850 nm central wavelength to compensate for the time delay required in the reference arm. The waveguides used in our structure are based on $Si_3N_4$and SiO_2technology called Triplex.We preferred channel buried waveguide geometry to achieve low propagation losses and better mode confinement. Smaller bending radius is required to miniaturize the device, so we encapsulated Si_3N_4 between SiO_2 layersdue to having medium refractive index contrast between$Si_3N_4(1.98)$ and $SiO_2(1.45)$. Schematic of waveguide structure is shown in Figure 1.

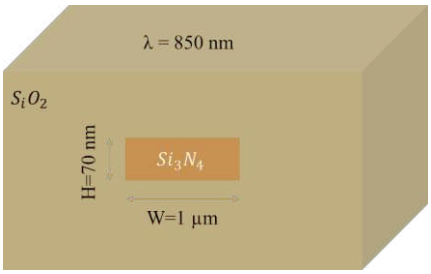

Fig:1: Illustration of channel buried waveguide at 850 nm wavelength

Reference delay lines for OCT prefer single mode operation as multimode might alter its axial resolution and sensitivity. To optimize the width and thickness of waveguide core for single mode operation, we have done modelling of waveguide using fully vectorial Finite Difference Mode (FDM) solver of Fimmwave simulation tool. Effective indices were calculated at the lower spectral end i.e. 750 nm of the broadband structure. The calculated effective indices for TE and TM mode as a function of waveguide core width (W) and thickness (H) are shown in Figure 2.

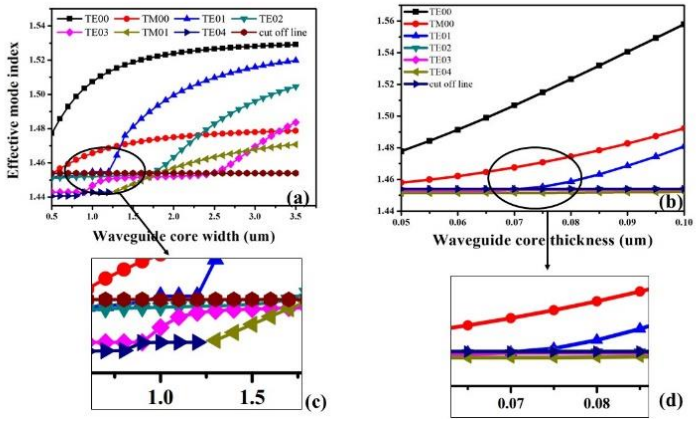

Fig:2: Mode effective index calculations of waveguide core (a) width and (b) thickness for TE and TM modes at 750 nm wavelength

It has been observed from the figure 2(a) that for waveguide core width below 1.2 µm only fundamental TE and TM mode will propagate. Also, from figure 2(b) it can be viewed that fundamental TE and TM modes will propagate for waveguide core thickness below 75 nm. So, after analysis of results, the width and thickness for single mode operation are optimised as 1 µm and 70 nm respectively.

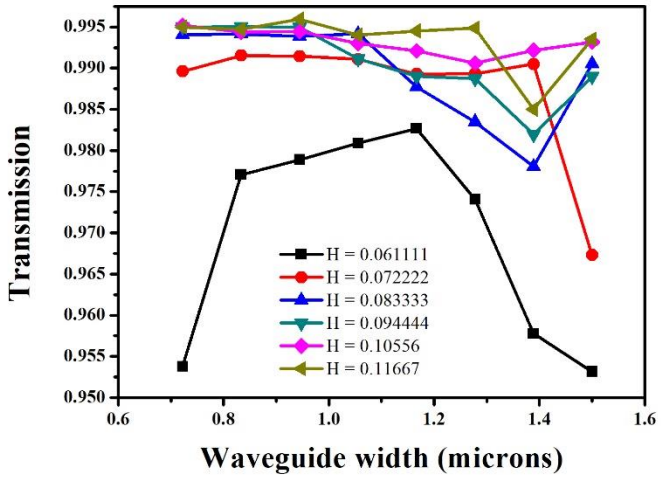

Fig 3: Normalized transmission over waveguide core width and thickness at 850 nm wavelength

Once we have achieved cut off value of waveguide core W and H, transmission below these values is an essential factor which needs to be contemplated. For this we have considered values of W ranging from 0.7 um to 1.4 µm and H ranging from 0.05 µm to 0.09 µm. A plot of waveguide W and H vs transmission at output is shown in Figure 3. It can be interpreting from the graph that best suitable values for maximum transmission below cut-off will be for W greater than 0.9 µm and H greater than 0.065 µm. So, after analysis of results, the W and H for single mode operation with transmission efficiency are optimised as 1 µm and 70 nm respectively.

3. Spiral Reference Section Design

The reported spiral delay line has been constructed using interleaved Archimedean spiral with continuous change of bending radius. General descriptive schematic for spiral reference delay line at 850 nm is shown in Fig 4. The reported structure covers an area of approximately 6×6 sq. mm.

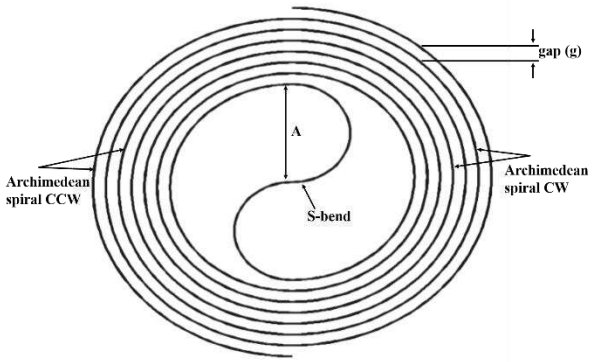

Figure 4: Descriptive illustration of reported spiral reference delay line

The structure consists of 2 set of half circles of which one set is used to bring light into the centre and other outwards towards the output. These inwards and outwards semi circles are connected to a S bend shaped structure whose radius is kept adiabatically large enough so as to have lossless transmission and change of mode location between CW and CCW spiral waveguides. Design parameters and propagation characteristics were modelled and optimized using Eigen Mode Expansion (EME) method of Fimmprop. Circular bends with a bend section along the circular path were used for designing the structure. The structure began with a set of bending arcs having 180° phase shift each for CW rotation. Each successive bending arc was set with a decreasing radius so as to form an inward spiral. A total 30 set of semi-circular bending arcs were used to form this inward spiral. Next an S-bend section was designed using two bending arcs of same radius having +180° and -180° phase shift each. The bending

section exiting the S-bend was then connected through a set of bending arcs having -180° phase shift with increasing radius for all successive arcs.

The minimum bending radius is a very significant parameter as the overall length of spiral is dependent on it. For the optimization of minimum bending radius, we have calculated the transmission and excess loss over a range of 0.5 mm to 3.5 mm. Results obtained for variation in transmission and excess loss vs bending radius is plotted in Figure 5.

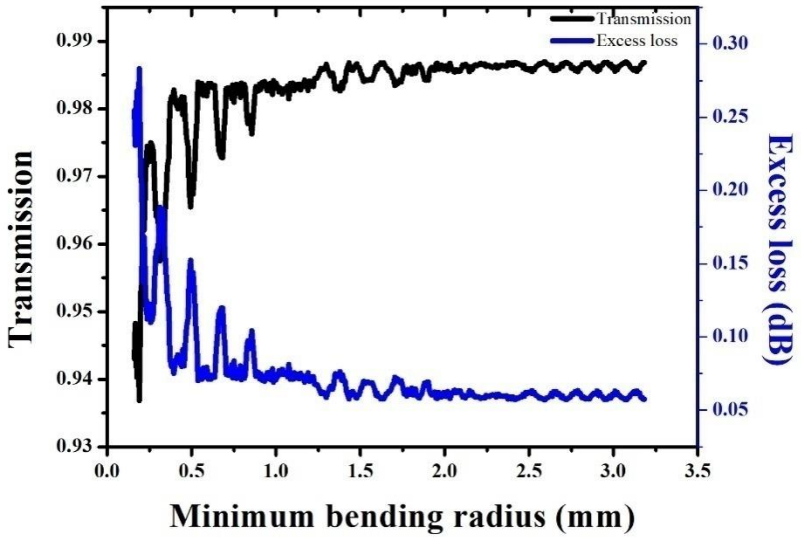

Fig. 5: Min. bending radius vs power at output

From Fig.5, it has been observed that the first constant maximum was achieved at 1.29 mm, next at 1.47 mm and then at 1.66 mm bending radius and so on. We have considered 1.47 mm as minimum bending radius as at 1.47 mm, the reported structure results with minimum excess losses for a broad range (200 nm) of spectrum.

Mathematical calculations

The length of consecutive semi circles is then related to the length of minimum bending arc by following relation.

$$A2 = (A \times 2) + dA \quad (1)$$

Where A is the minimum bending arc length and dA is 10 µm and $A2$ is the bending arc length of consecutive semi-circle from S bend.

A multiplication factor of 2 was used for consecutive bending radius as S-bend was constructed using two bending arcs. So the next bending arcs should be wide enough such that overlapping doesn't occur. Moreover, a value of 10 µm was also added along with the multiplication factor so that coupling between consecutive arcs doesn't take place.

In general, there is a need for very accurate length parameters to be specified. Although this can be altered later on by few modifications in some parameters. The number of semi-circular arcs is mainly responsible for the overall length of spiral. For this structure, the number of half circles are taken to be 30 i.e. 30 half circle are deployed both in CW and CCW direction and the relation of each arc length can be determined by following relation

$$A_n = A_{n-1} + 10; \ for\ n = 3\ to\ 30 \quad (2)$$

Once the length of each half arc is being determined, the overall length (L) of spiral structure can then be defined by following relation as

$$L = 2 \times \sum_{n=1}^{30} A_n \quad (3)$$

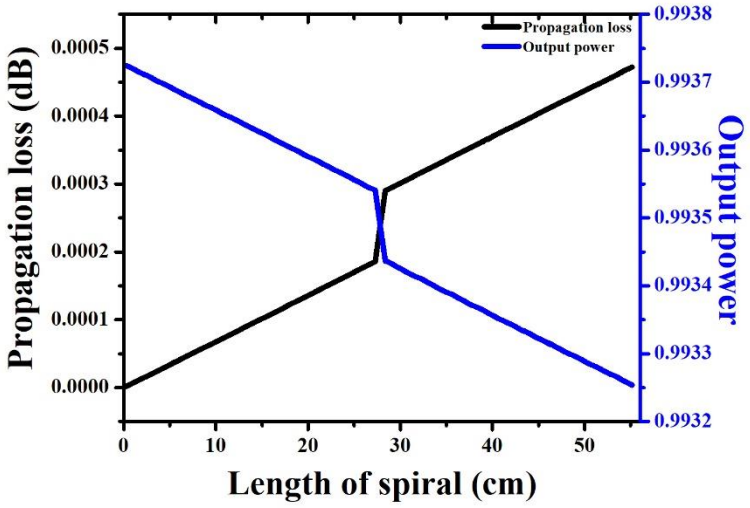

Fig.6: Length of propagation at 850 nm wavelength

Spiral structure results

For minimum bending radius of 1.47 mm, an overall delay line of 55.11 cm is accounted. The relation between length of propagation across spiral structured delay line vs power obtained and loss can be seen in Fig. 6. The overall propagation loss across the length of propagation was 0.00047 dB.

The time delay can then can be calculated by following relation

$$t_d = \frac{n_g \times L}{C} \qquad (4)$$

Where t_d is the time delay of the spiral delay line, n_g is the group effective index and C is the speed of light. For a delay length (L) of 55.11 cm and effective group index (n_g) of 1.62 (TE mode) and 1.51 (TM mode), a delay time of 2.35 ns and 2.19 ns is reported for this structure at 850 nm.

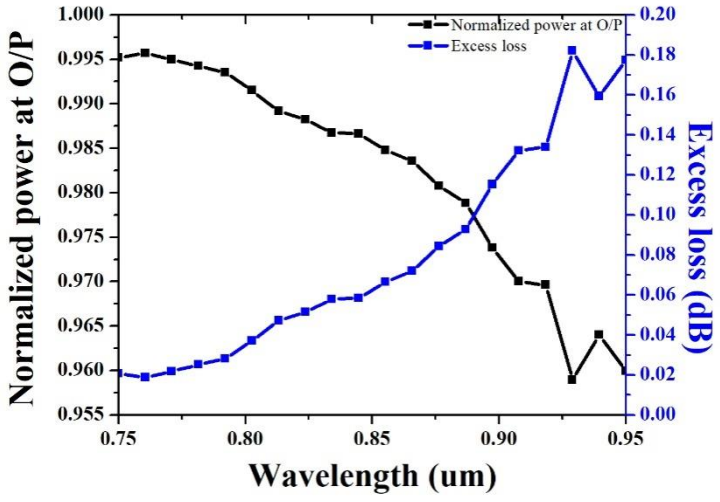

Fig. 7: Normalized power at output and excess loss for 200 nm bandwidth at 850 nm central wavelength

Now in order to analyse the structure performance, certain parameters such as its bandwidth, normalized power at output and excess loss are to be determined. The reported structure has been scanned over 200 nm i.e. from 750 nm to 950 nm at 850 nm central wavelength and is found to be broadband over this bandwidth range. Also, at 850 nm central wavelength, a normalized power of 98.64% and an excess loss of 0.06 dB is accounted. A maximum excess loss of 0.18 dB is observed across 200 nm bandwidth. The relation between bandwidth, normalized power and excess loss at 850 nm centre wavelength can be seen through Fig. 7.

2.3 Performance Analysis for TE, TM and FV modes

The calculations for the reported structure as stated above were performed for fully vectorial (FV) mode type which consists of both TE and TM modes. Now in order to study the individual mode performance for reported structure it is important to study the structural behaviour at TE and TM modes individually. Certain calculations were performed at different bending radius for all three mode types and analysis for the same is reported in Table 2. It can be seen from the calculations that for FV mode types, a constant PL is observed at all bending radius values.

For TE mode, it can be seen that an reduces PL occurs on increasing the bending radius value. A reduced PL of 0.000411dB for spiral structure length of 83.56 cm resulting a delay of 3.56 ns. The PL can be seen to be constant thereafter for spiral length of 86.06 cm, 94.30 cm and 96.88 cm resulting in a corresponding time delay of 3.67 ns, 4.02 ns and 4.13 ns respectively.

For TM mode, it is observed that for even smaller values of bending radius, reduced PL takes place. At spiral length of 14.67 cm a PL of 0.0042 dB was observed resulting in a time delay of 0.61 ns. Moreover, for increasing spiral length values, reduced PL is observed.

It can be analysed that TM mode shows best performance in comparison to other mode types while TE mode shows better performance than FV mode. The reduced performance for TE mode in comparison to TM mode may attribute due to sidewall roughness at waveguide core.

Table 1: Performance analysis for TE, TM and FV modes

Mode type	Min. bend. radius (mm)	L of spiral (cm)	Td (ns) TE	Td (ns) TM
FV	1.48	55.11	2.35	2.19
	1.66	61.88	2.64	2.46
	1.79	66.60	2.84	2.65
	1.84	68.25	2.91	2.72
	2.16	80.29	3.43	3.20
	2.41	89.38	3.81	3.56
	2.73	101.07	4.31	4.02
	3.08	112.65	4.81	4.49
TE	1.62	59.73	2.55	-
	1.81	66.74	2.85	-
	2.28	83.56	3.57	-
	2.34	86.06	3.67	-
	2.57	94.30	4.03	-
	2.64	96.88	4.14	-
TM	0.38	14.67	-	0.61
	0.72	27.41	-	1.14
	1.01	38.04	-	1.59
	1.78	51.96	-	2.17
	2.01	74.51	-	3.11
	2.23	82.89	-	3.46

3 Tolerance Analysis

The design tolerance was calculated at ±2% deviation for waveguide core width and thickness. The simulations for design tolerance were performed for FV mode type in terms of EL and PL parameters. The EL calculations were performed for 200 nm wavelength range which can be seen through Figure 8. It is observed from the plot that the maximum EL of 0.27 dB is accounted which is little higher than the original EL of 0.17 dB. Also, at 850 nm, an almost similar EL of 0.06 dB was observed for all deviation in width and thickness

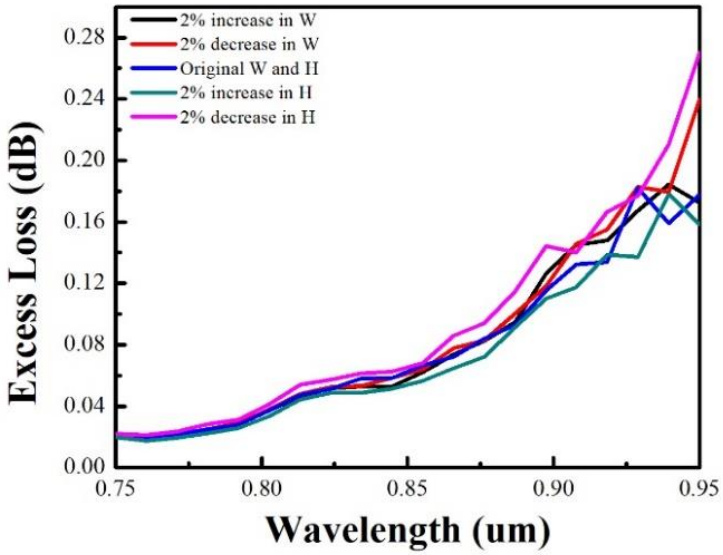

Fig. 8: Tolerance analysis for EL at 850 nm

Next PL was calculated at ±2% deviation for waveguide core width and thickness. The plot for PL in terms of its design tolerance can be seen through Figure 8. It can be seen that a constant PL was observed for entire length of propagation at all deviations in waveguide width and thickness at 850 nm central wavelength.

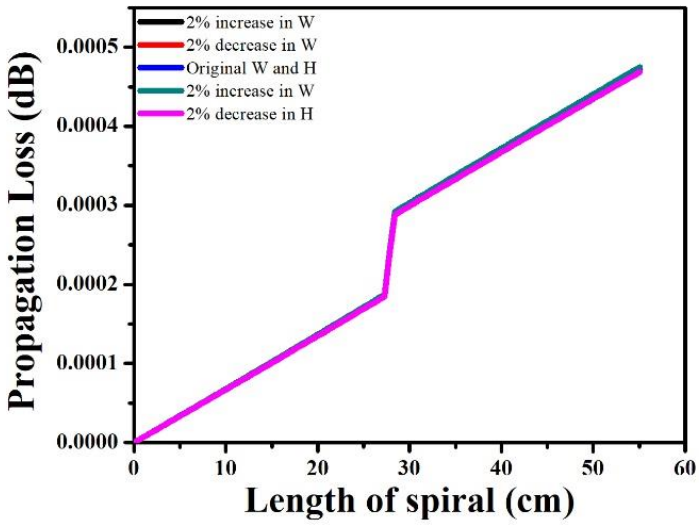

Fig. 9: Tolerance analysis for PL at 850 nm

It can be thus be analysed from Figure 8 and 9 that the reported structure is fabrication tolerant and can be used for IO based OCT systems.

The reported structure was also compared to some of the existing structure available in literature. A comparison analysis can be seen through Table 3. For Si_3N_4 material-based delay line structures, a time delay of 395 ps and 17.2 ns was observed with a loss of 3.6 dB and 0.5 dB respectively. It can be observed from the table that lowest PL was calculated for the reported spiral delay line with a compact footprint of only 6×6 mm sq. It lists the comparison of this reported spiral delay line with various state of art integrated optical delay lines over the years. Comparisons are made in terms of loss obtained, delay time acquired, material and wavelength used, length of delay structure and area occupied and bandwidth. To the author's knowledge, this is the first ever attempt to design an integrated spiral delay line at 850 nm wavelength using Si_3N_4 / SiO_2material.

Table 2: Comparison of various optical delay lines from literature and reported structure

Paper	Loss	Delay	Material	Wavelength	Length	Area
Dongdong Lin (2019)	3.6 dB	395 ps	Si_3N_4	40 GHz	NA	6.4×2 sq mm
Bykhovsky (2018)	0.5 dB	17,2 ns	Si_3N_4	1.55 um	2.59 m	17.7 mm wafer size
Yan Li(2016)	37.7dB IL/ 1.908dB/cm	2.804 ns	SOI	1.55 um	19.79 cm	1×1 mm
Chen (2015)	2.5 dB/cm	NA	Si/SiO_2	1.55 um	4 mm	0.13 ×0.13 sq mm
Chen,(2014)	0.1dB/m	NA	Si/SiO_2	NA	7m	9.5 ×9.5 sq mm
Yurtsever (2014)	NA	NA	Si_3N_4 $/SiO_2$	1320 nm	190 mm	10×33 sq mm
JingyaXie (2014)	16 dB IL, 0.013 dB/ps delay loss	1.27 ns	Si	1.55 um	NA	11.84 sq mm
Cherchi,(2014)	0.15dB/cm	NA	SOI	1.55 um	2.8 cm	NA
Stopinski(2013)	10 dB	250 ps	InP	1.55 um	2 cm	0.38 sq mm
Hansuek Lee,(2012)	0.037 dB/m	NA	Si	1570 nm	27 m	NA
This work	**0.00047 dB PL 0.18 dB IL**	**2.35 ns/ 2.19 ns**	$\boldsymbol{Si_3N_4}$ $\boldsymbol{/SiO_2}$	**850 nm**	**55.11 cm**	**6×6 sq mm**

Where IL=Insertion loss, PL=Propagation loss

4. Conclusion

In this work, design and simulation of compact spiral delay line for application as parameterized building block in integrated optics-based OCT has been presented. Simulation results show a potential of Si_3N_4 / SiO_2 material to be used for further integration of other components in OCT system. The reported delay line showed very promising results over 200nm bandwidth at 850 nm central wavelength. Over the length of propagation of 55.11 cm, an excess loss of 0.06 dB and propagation loss of 0.027 dB was accounted in an area of 6×6 sq. mm. Also, the design was analysed for TE, TM and FV mode types and their performance comparison shows TM mode to be the best candidate. The structure was also analysed in terms of its tolerance parameter and was found to be design tolerant. With further optimization with directional coupler, the system will replace the beam splitters in existing fibre optics-based OCT system.

ACKNOWLEDGEMENT

This work is supported by DIT University, Dehradun, India. The authors would like to thank Vice-chancellor and management of DIT University, India, for encouragement and support during the present research work. The authors are also thankful to Dr. Sulabha Ranade, Director General, SAMEER and Sh. S.S. Prasad, Programme Director, SAMEER for their encouragement and support for this work. One of the authors Dr. Kamal Kishor, would also like to gratefully acknowledge the financial support provided by the TIFAC-Centre of Relevance and Excellence in Fiber Optics and Optical communication at Delhi Technological University (Formerly Delhi College of Engineering, Delhi) through the Mission Reach program of Technology, Vision-2020, Government of India.

Declaration:

The authors declare no conflict of interest.

References

[1] Yadvendra Singh, Sanjeev K. Raghuwanshi, Manish Kumar, "Photonic based liquid level transmitter using Mach-Zehnder interferometer for industrial application," Proc. SPIE 10539, Photonic Instrumentation Engineering V,105391A (22 February 2018); doi: 10.1117/12.2289616.

[2] Srivastava N. K., R. Parihar and S. K. Raghuwanshi, "Efficient Photonic Beamforming System Incorporating a Unique Featured Tunable Chirped Fiber Bragg Grating for Application Extended to the Ku-Band," in *IEEE Transactions on Microwave Theory and Techniques*, vol. 68, no. 5, pp. 1851-1857, May 2020, doi: 10.1109/TMTT.2019.2961889.

[3] Fercher A. F., W. Drexler, C. K. Hitzenberger, and T. Lasser, "Optical coherence tomography-principles and applications," *Reports on Progress in Physics*, vol. 66, pp. 239–303, 2003. https://doi.org/10.1088/0034 4885/66/2/204

[4] Izatt, J. A., &Choma, M. A. (2008). Theory of Optical Coherence Tomography (book chapter), 47–72. https://doi.org/10.1007/978-3-540-77550-8_2

[5] Shahoei, Hiva & Yao, Jianping. (2014). Delay Lines.(book chapter) 10.1002/047134608X.W8234.

[6] Sharma T. et al., "Design of grating based narrow band reflector on SOI waveguide," Optik (Stuttg)., p.p 165995, 2020, doi: 10.1016/j.ijleo.2020.165995.

[7] Zhou, L., Wang, X., Lu, L., & Chen, J. (2018). Integrated optical delay lines: a review and perspective [Invited]. *Chinese Optics Letters*, *16*(10), 1–16. https://doi.org/10.3788/COL201816.101301

[8] Watcharakitchakorn, O., &Silapunt, R. (2018). Design and modeling of the photonic crystal waveguide structure for heat-Assisted magnetic recording. *Advances in Materials Science and Engineering*, *2018*. https://doi.org/10.1155/2018/8097841

[9] Stopinski, S., Malinowski, M., Piramidowicz, R., Kleijn, E., Smit, M. K., &Leijtens, X. J. M. (2013). Integrated optical delay lines for time-division multiplexers. *IEEE Photonics Journal*, *5*(5). https://doi.org/10.1109/JPHOT.2013.2280519.

[10] Yurtsever, G., Považay, B., Alex, A., Zabihian, B., Drexler, W., &Baets, R. (2014). Photonic integrated Mach-Zehnder interferometer with an on-chip reference arm for optical coherence tomography. *Biomedical Optics Express*, *5*(4), 1050. https://doi.org/10.1364/boe.5.001050

[11] Waqas, A., Melati, D., &Melloni, A. (2018). Cascaded Mach-Zehnder architectures for photonic integrated delay lines. *IEEE Photonics Technology Letters*, *30*(21), 1830–1833. https://doi.org/10.1109/LPT.2018.2865703

[12] Lin, D., Xu, X., Zheng, P., Yang, H., Hu, G., Yun, B., & Cui, Y. (2019). A Tunable Optical Delay Line Based on Cascaded Silicon Nitride Microrings for Ka-Band Beamforming. *IEEE Photonics Journal*, *11*(5), 1–10. https://doi.org/10.1109/jphot.2019.2941510

[13] Sharma, B., Kishor, K., Sharma, S., & Makkar, R. L. (2019). *Broadband SiN directional coupler at 850 nm for optical coherence tomography*. (September), 31. https://doi.org/10.1117/12.2529351

[14] Sharma, B., Kishor, K., Sharma, S., & Makkar, R. (2019). Design and Simulation of Broadband Beam Splitter on a Silicon Nitride Platform for Optical Coherence Tomography. *Fiber and Integrated Optics*, *0*(0), 1–11. https://doi.org/10.1080/01468030.2019.1639001

[15] Chen, T., Lee, H., Li, J., Painter, O., &Vahala, K. (2011). Ultra-low-loss optical delay line on a silicon chip. *Optics InfoBase Conference Papers*, *3*(May), 867. https://doi.org/10.1038/ncomms1876

[16] Xie, J., Zhou, L., Li, Z., Wang, J., & Chen, J. (2014). Seven-bit reconfigurable optical true time delay line based on silicon integration: erratum. *Optics Express*, *22*(21), 25516. https://doi.org/10.1364/oe.22.025516

[17] Chen, T., Lee, H., &Vahala, K. J. (2014). Design and characterization of whispering-gallery spiral waveguides. *Optics Express*, *22*(5), 5196. https://doi.org/10.1364/oe.22.005196

[18] Cherchi, M., Ylinen, S., Harjanne, M., Kapulainen, M., Vehmas, T., & Aalto, T. (2014). Low-loss spiral waveguides with ultra-small footprint on a micron scale SOI platform. *Silicon Photonics IX*, *8990*, 899005. https://doi.org/10.1117/12.2039940

[19] Chen, Z., Flueckiger, J., Wang, X., Zhang, F., Yun, H., Lu, Z., … Chrostowski, L. (2015). Spiral Bragg grating waveguides for TM mode silicon photonics. *Optics Express*, *23*(19), 25295. https://doi.org/10.1364/oe.23.025295

[20] Li, Y., Song, X., Xu, Y., & Li, Y. P. (2014). Spiral optical delay lines in silicon-on-insulator. *Optics InfoBase Conference Papers*, (2), 3–5. https://doi.org/10.1364/ACPC.2016.AF3G.6

[21] Bykhovsky, D., Rosenblit, M., &Arnon, S. (2018). Two-sided through-wafer interconnect for optical spiral delay line. *Journal of Modern Optics*, *65*(1), 98–103. https://doi.org/10.1080/09500340.2017.1377305

[22] Li, W., Anantha, P., Lee, K. H., Qiu, H. D., Guo, X., Goh, S. C. K., … Tan, C. S. (2018). Spiral Waveguides on Germanium-on-Silicon Nitride Platform for Mid-IR Sensing Applications. *IEEE Photonics Journal*, *10*(3), 1–7. https://doi.org/10.1109/JPHOT.2018.2829988

[23] Moralis-Pegios, M., Mourgias-Alexandris, G., Terzenidis, N., Cherchi, M., Harjanne, M., Aalto, T., … Vyrsokinos, K. (2017). On-ChipSOI delay line bank for optical buffers and time slot interchangers. *IEEE Photonics Technology Letters*, *30*(1), 31–34. https://doi.org/10.1109/LPT.2017.2773146

Figures

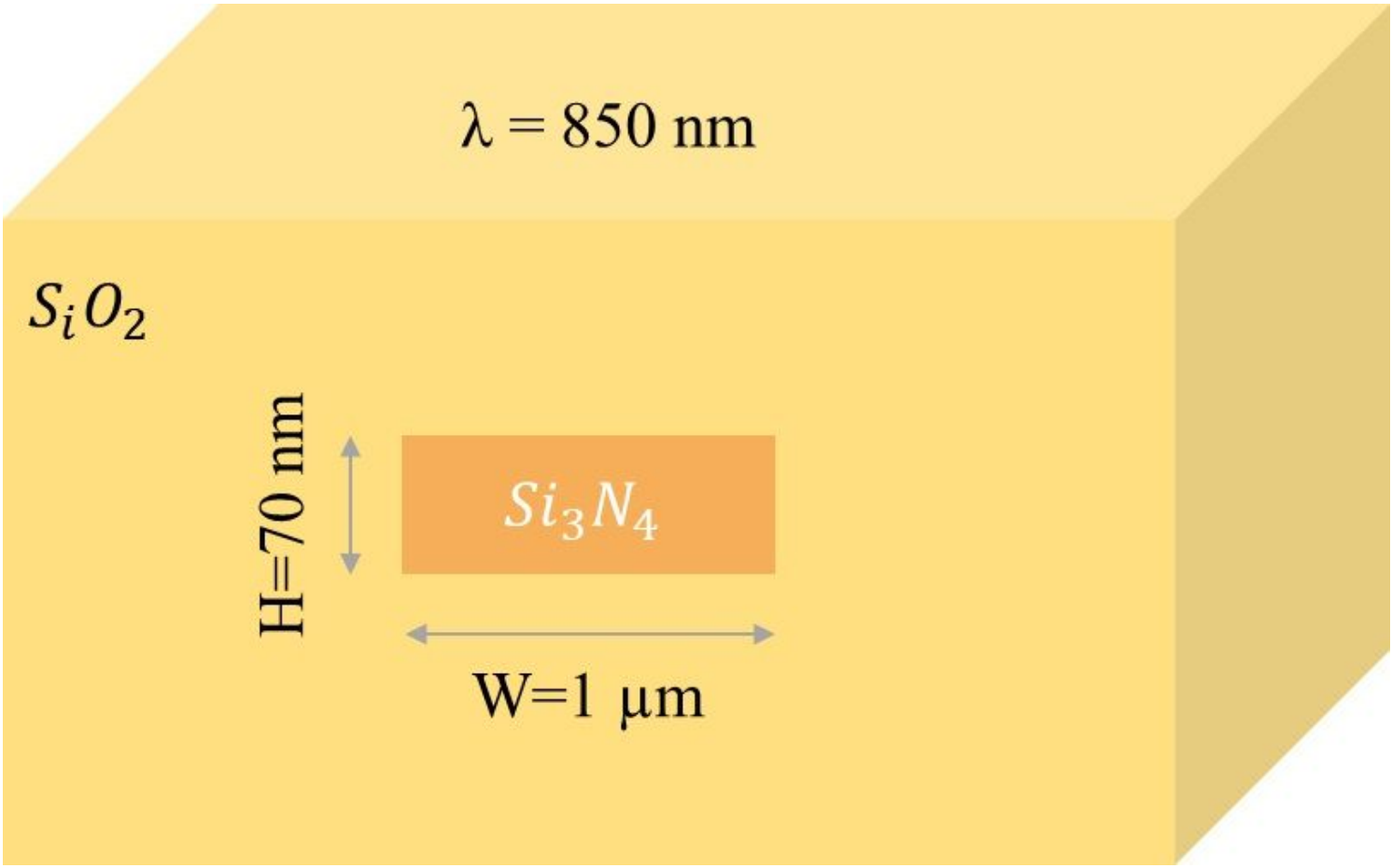

Figure 1

Illustration of channel buried waveguide at 850 nm wavelength

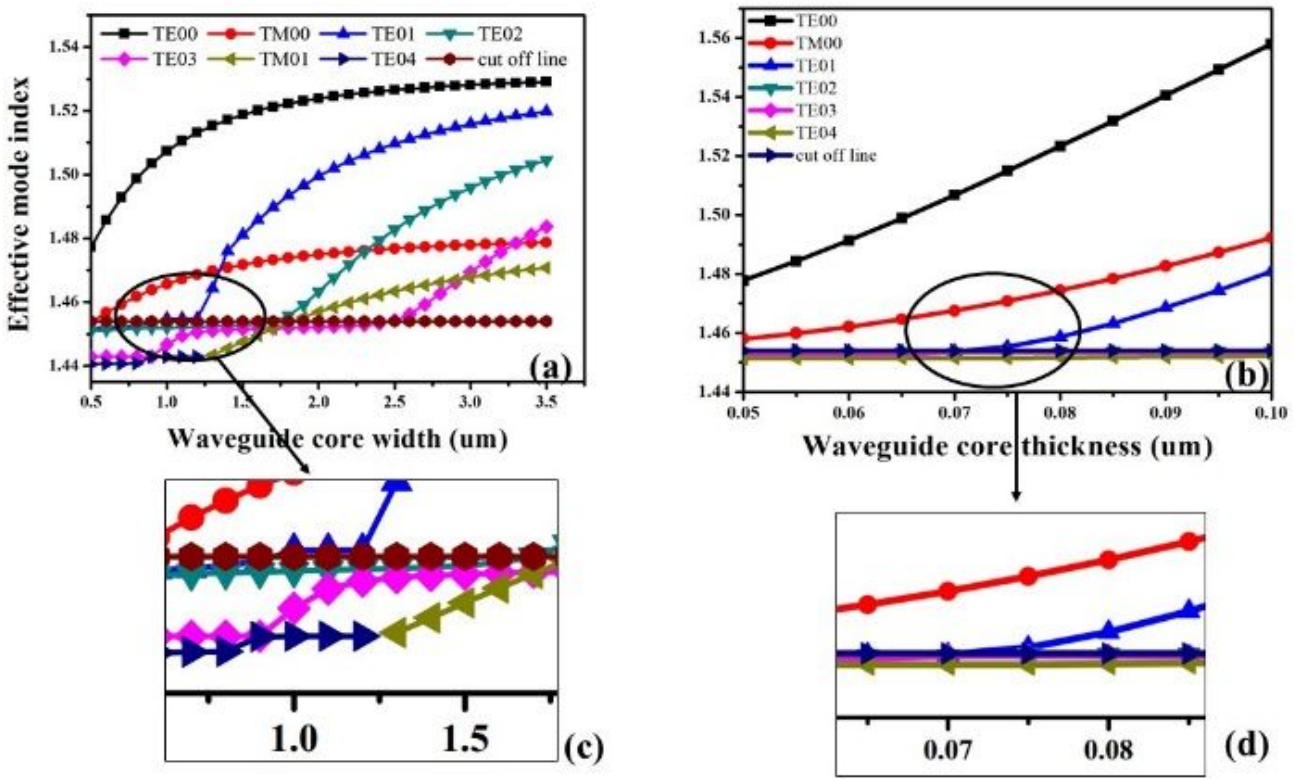

Figure 2

Mode effective index calculations of waveguide core (a) width and (b) thickness for TE and TM modes at 750 nm wavelength

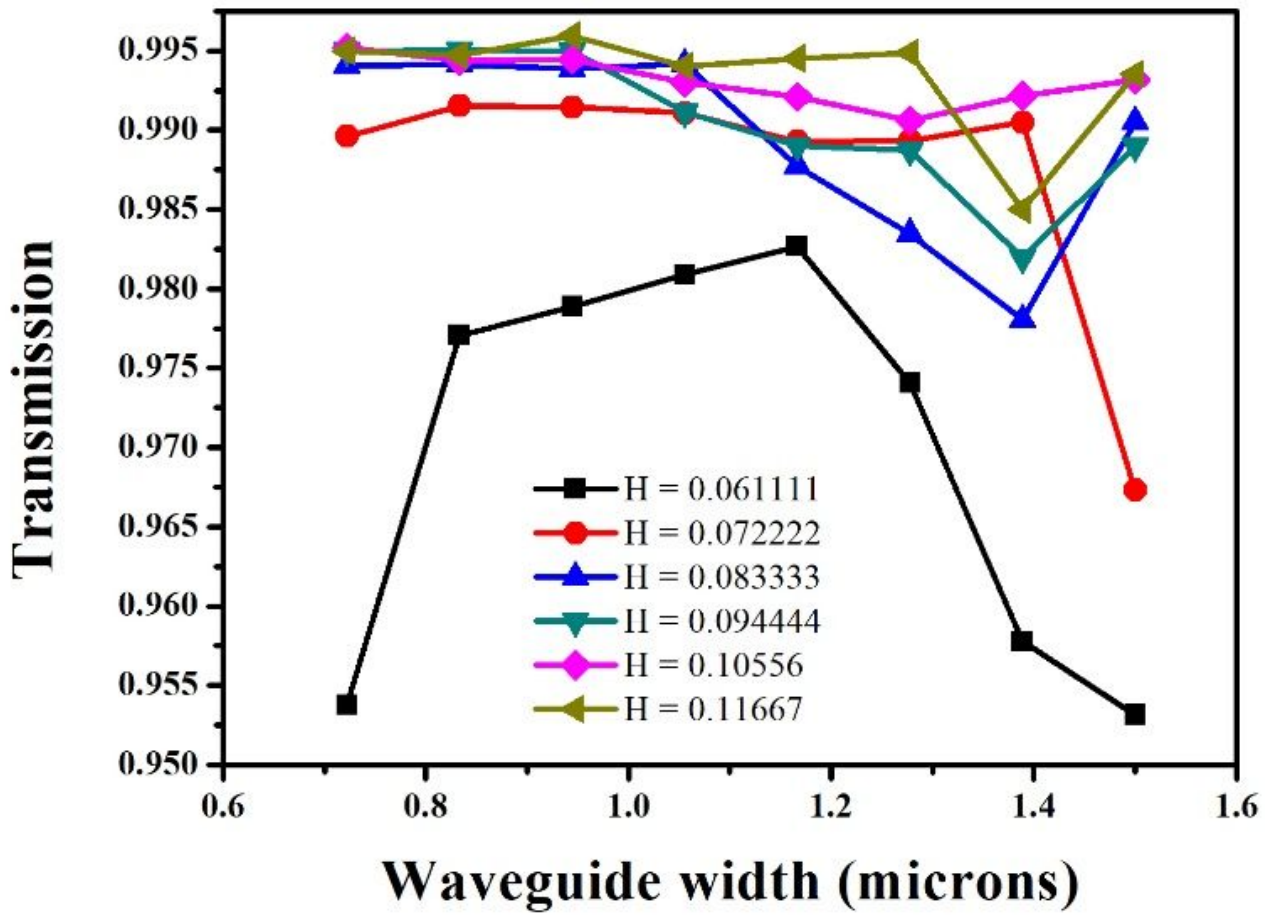

Figure 3

Normalized transmission over waveguide core width and thickness at 850 nm wavelength

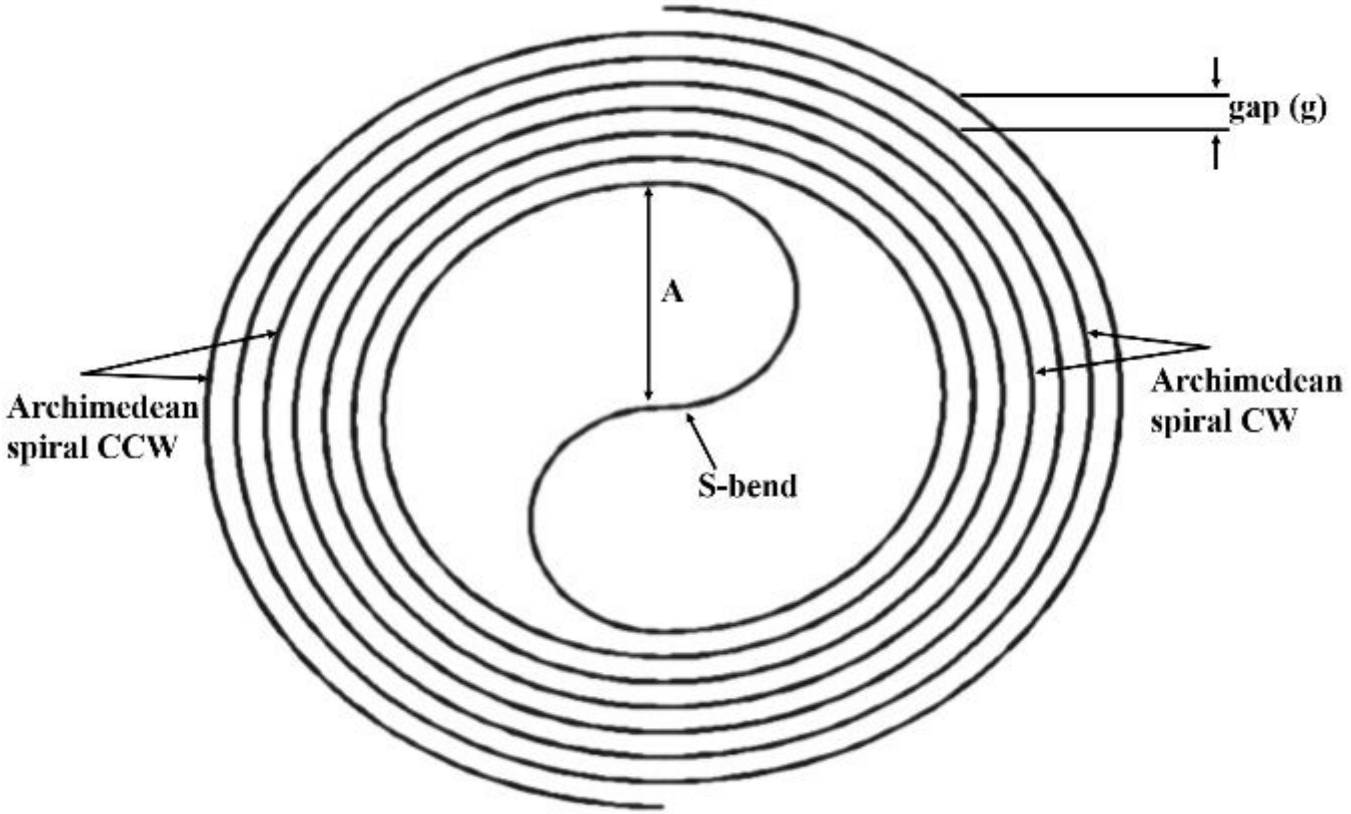

Figure 4

Descriptive illustration of reported spiral reference delay line

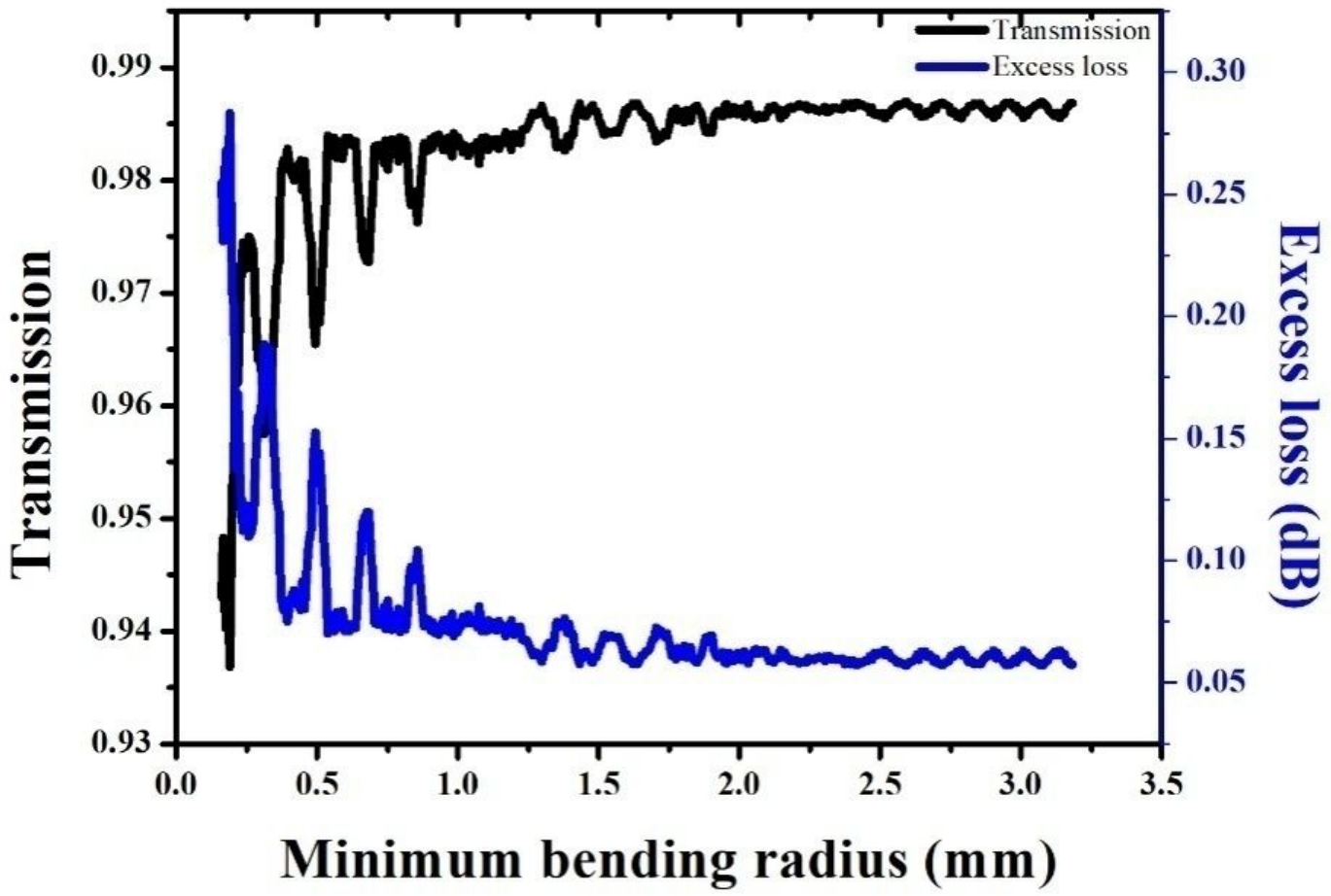

Figure 5

Min. bending radius vs power at output

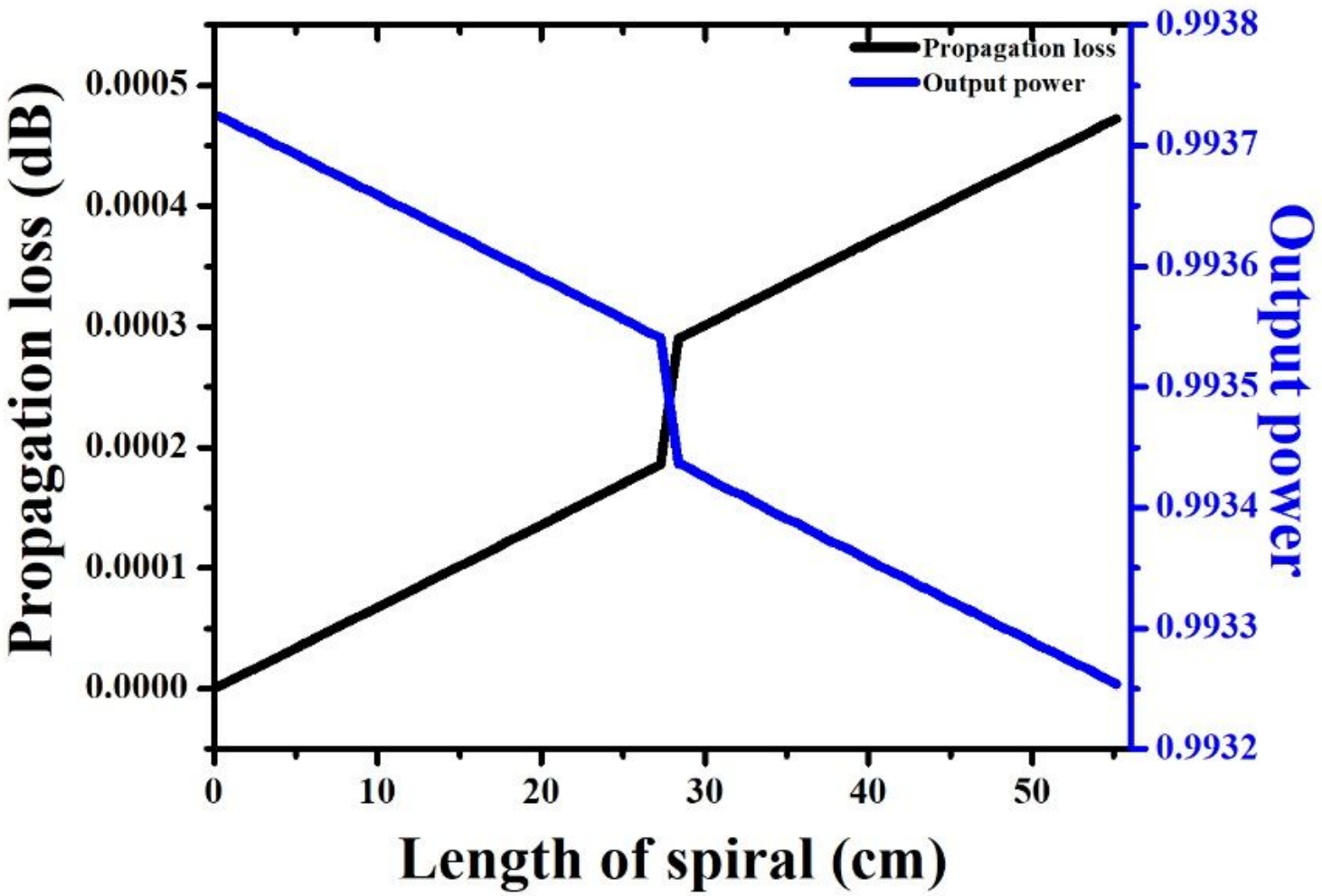

Figure 6

Length of propagation at 850 nm wavelength

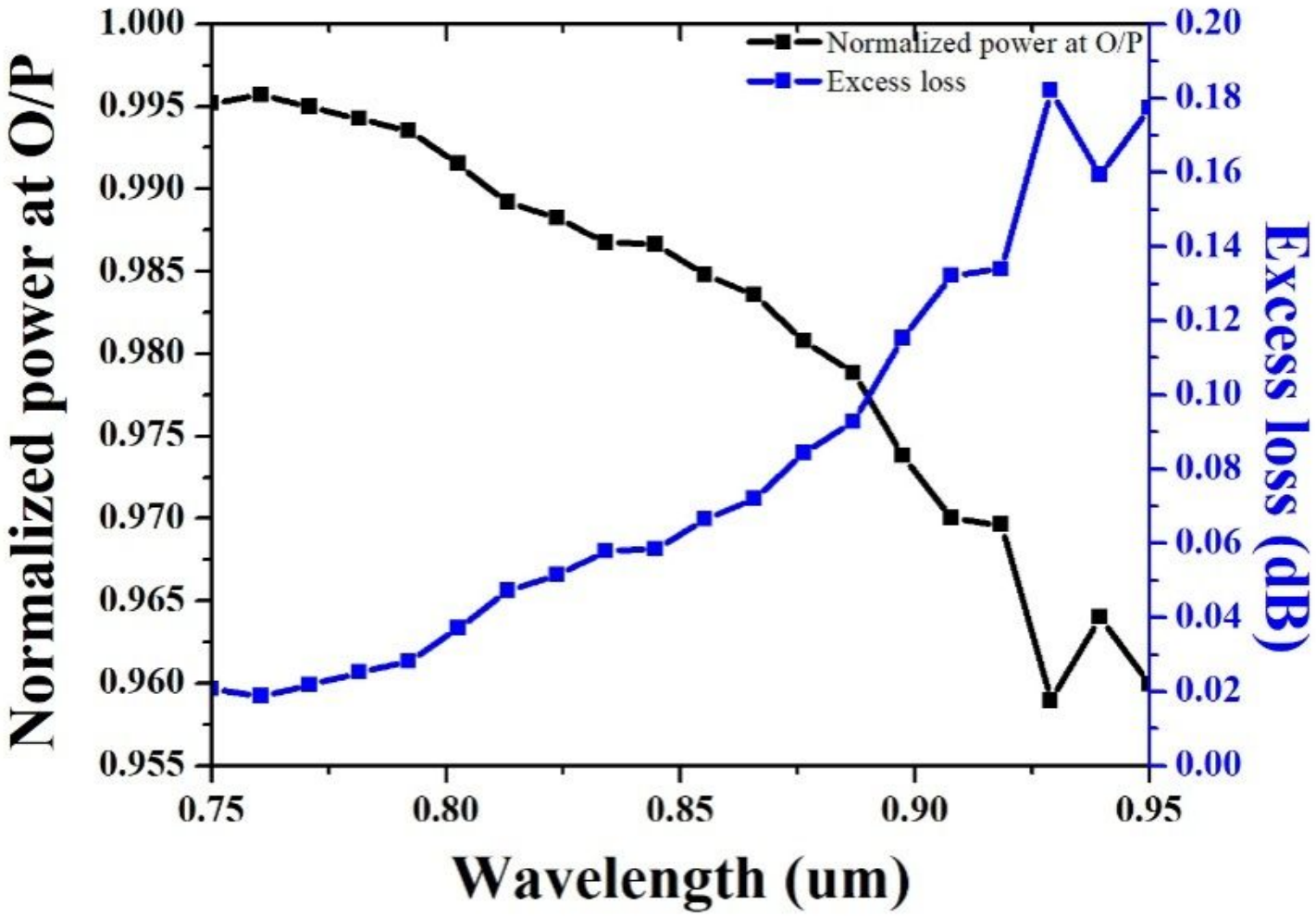

Figure 7

Normalized power at output and excess loss for 200 nm bandwidth at 850 nm central wavelength

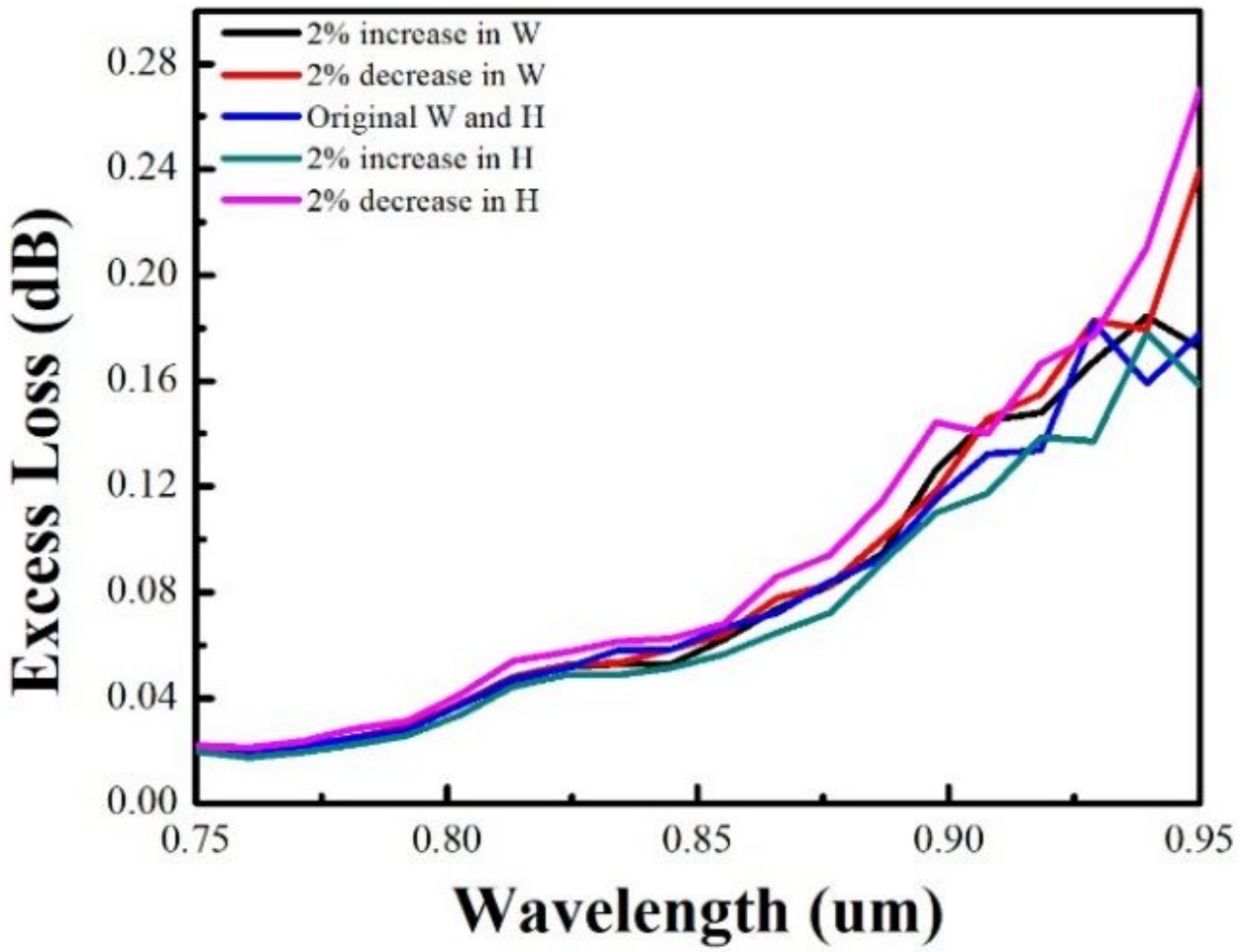

Figure 8

Tolerance analysis for EL at 850 nm

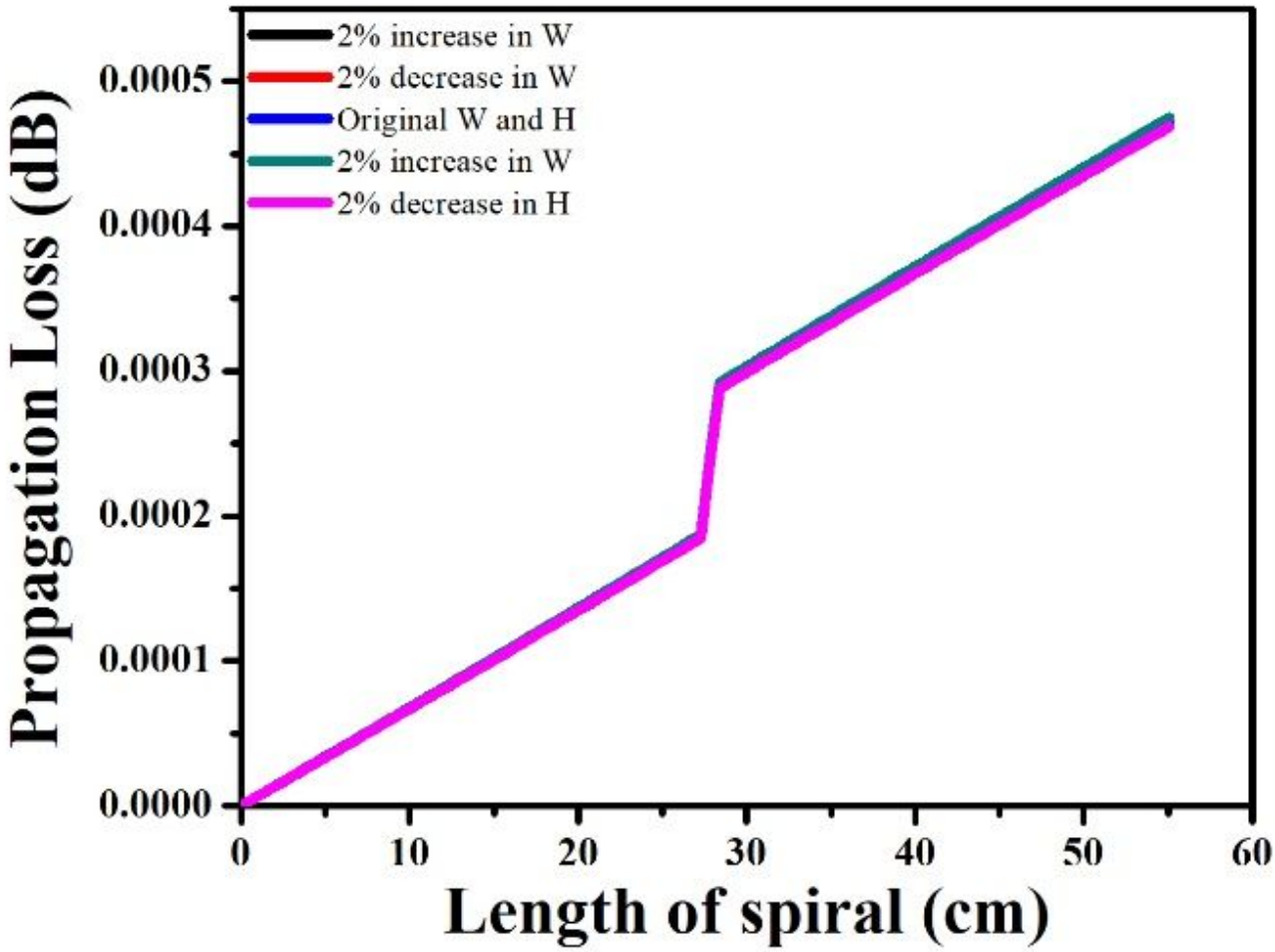

Figure 9

Tolerance analysis for PL at 850 nm